3. RESULTS AND DISCUSSION

3.1 Preparation of active carbons

The preparation of activated carbon was done either by physical or chemical activation. The total samples prepared from activated carbons were four samples.

Table (3.1) preparation conditions of active carbons

No	Sample notation	Preparation conditions
1	OS N – 1850	Activation using steam / N_2 gas at 850 ^oC for 1 h
2	OS P_{60} – 2500	Activation using 60% H_3PO_4 at 500 ^oC for 2 h
3	OS P_{70} – 2500	Activation using 70% H_3PO_4 at 500 ^oC for 2 h
4	OS P_{80} – 2500	Activation using 80% H_3PO_4 at 500 ^oC for 2 h

3.2. Characterization of the prepared carbons

3.2.1. Bulk density (Packed density)

The density of the final products after activation depends not only on the nature of the starting material but also on the activation process [97].

The experimental results of the bulk density of physical and chemical activated olive stones are represented in Table (3.2). In physical activation, it is clear that, sample OSN-1850 has less bulk density (0.671 g/cc) due to the fact that , the changes in densities are related to the reaction rate between carbon and steam, which

essentially depends on the reaction time and activation temperature. Evidently, with increasing time of activation process, there is successive release of volatiles, gases, and oil or tars; consequently, the steam penetrates easily into the surface of olive stone .

Samples of OSP_{60}-2500; OSP_{70} – 2500 and OSP_{80}- 2500 are prepared from olive stone through chemical activation, produced activated carbons with high density, in the range of 0.776 - 0.833 g /c.c. Table (3.2).

In practical terms, granular activated carbons (GACs) with high bulk densities are preferred for general use. The American Water Works Association (AWWA) has set a lower limit of the bulk density at 0.25 g/c.c. for GACs to be of practical use [98]. Accordingly, all of the four carbons prepared from olive stones either by physical or chemical activation, would fall within this guideline.

3.2.2. pH

The pH of the carbon is an important parameter of interaction between the adsorbate containing fluid and the carbon, which contain other non-carbonceous constituents[99,100]. The surface chemical nature of the prepared adsorbents was estimated by measuring their pH. The obtained data are presented in Table (3.2).

Hassler [101] reported that the pH of most commercial activated carbons is due to inorganic constituents (ash) originating from the precursor or added during manufacture. In this concern, table (3.2) shows that the chemical activation using H_3PO_4 gives activated carbon

with pH < 4 for the samples (OS P_{60} – 2500 , OS P_{70} – 2500 and OS P_{80} – 2500). This means that some phosphours oxides and / or phosphate groups are penetrated during activation to the cellular structure and lowers the pH of these carbons. Consequently, it was possible to prepare acidic (H_3PO_4) and basic(N_2) carbons from olive stone to check their adsorbability for THMs removal.

Table (3.2) Bulk Density and pH measurements of activated carbons

Sample Notation	Bulk Density (g/ml)	pH
OSN – 1850	0.6713	10.4
OS P_{60} – 2500	0.776	2.07
OS P_{70} – 2500	0.8481	2.6
OS P_{80} – 2500	0.833	3.15

3.2.3. Identification of Surface Functional Groups by The FT- IR specta

The FT- IR spectra of the prepared activated carbons derived from olive stones were carried out in the range 500-4000 cm^{-1} as shown in Fig. (3.1). The broad band centered at 3713 – 3683 cm^{-1} may be assigned to NH_2 stretching vibration of nitrile functional groups . The broad band centered at 3448 cm^{-1} can be assigned to O-H stretching vibration of hydroxyl functional groups [102]. The band around 2927 cm^{-1} are due to asymmetric and symmetric C-H stretching vibrations

in aliphatic –CH, -CH_2, -CH_3. Carbon-oxygen bands have been proposed to give bands around 1705 cm^{-1}, perhaps due to ketene or ketone [103]. A doublet bands appears: at 1627 cm^{-1} due to stretching vibrations of aromatic C=C bond, which are polarized by oxygen atoms near one of the carbon atoms[103]. The band appeared at 2367-2369 cm^{-1}may be due to stretching vibrations of triple bond C≡C bond. The band 2337 cm^{-1}may be due to weak nitrile group attached to aliphatic chain.

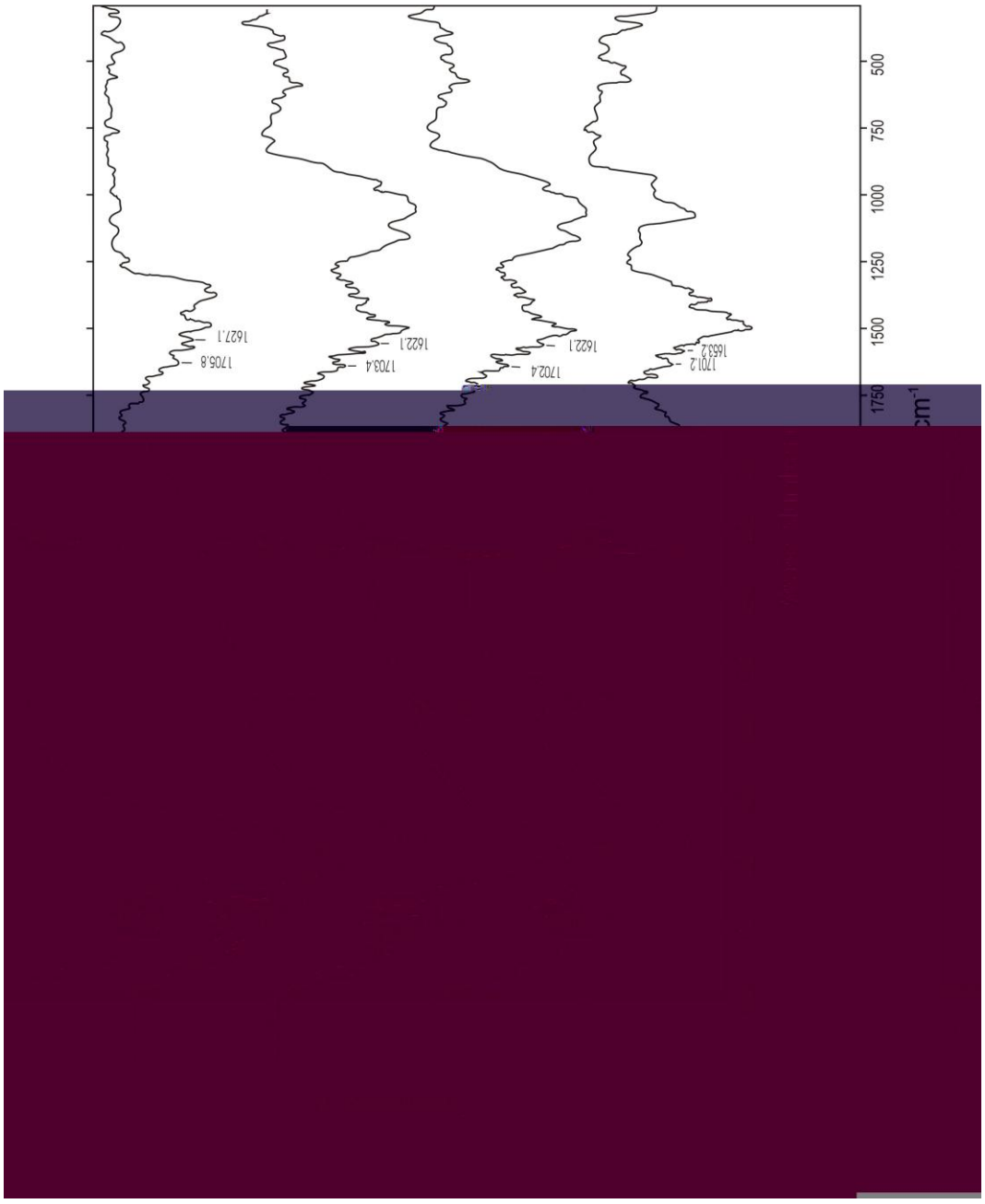

Fig (3.1) FT-IR spectra of prepared carbons

3.2. 4 Pore Structure Analysis.

Based on the results of low- temperature nitrogen adsorption isotherm the structure of the carbon was characterized using the BET equation in the range of relative pressure 0.05 up to 0.3 to calculate the apparent surface area (S_{BET}). The total pore volume (V_p) estimated from the amount of nitrogen adsorbed at relative pressure of 0.95 and the mean pore radius from $r_{BET} = 2 V_p / S_{BET}$ assuming cylindrical pore opens at both ends.

Table (3.3) Textural characteristics of the prepared activated carbons

Sample notation	S_{BET} m^2/g	$V_{mic.}$	V_p cm^3/g	V_{mic} / V_p %	$r = 2 V_p / S_{BET}$
OS N – 1850	748.9	0.2410	0.2466	97.8	0.0006
OS P_{60} – 2500	1230.2	0.3236	0.6301	51.4	0.001
OS P_{70} – 2500	1862.6	0.5602	0.8856	63.3	0.0009
OS P_{80} – 2500	2050.4	0.5854	1.0836	54	0.001

In case of physical activation using nitrogen gas as activating agent, the sample OSN -1850 has almost micropore structure 97.8% and its pore volume was 0.246 ml/g as shown in Table (3.3). Consequently, sample OSN -1850 is useful almost in removal of small pollutant molecules from water. Table (3.3) and Figs. (3.2) & (3.3) show the effect of phosphoric acid concentration (%) on porosity and pore structure development during the chemical activation of olive

stone. In this concern, it was clear that micro – and meso- pores formed by either 60 % or 80% are nearly equal. However, in case of sample OSP_{70}- 2500 prepared by 70% H_3PO_4 , there was apparent increase in micro pores. This proves that the sample OSP_{70}- 2500 is expected to be better than either sample OSP_{60}- 2500 or sample OSP_{80}- 2500 in uptake of smaller molecules. Consequently, both samples OSP_{60}- 2500 and OSP_{80}- 2500 are better in uptake of larger molecules of water pollutants in water treatment plants. Fig. (3.3) showed that the total pore volume, Vp, of the prepared samples are increased as the concentration of H_3PO_4 increases too giving significant increase in surface area. The commercial activated carbon on markets has almost total pore volume 1.0 cc/g and thus sample OSP_{80}- 2500 is the only sample that has comparable ,V_p, and is useful in wide applications . In general, the order of samples according to :

S_{BET} were: OSP_{80}- 2500 > OSP_{70}- 2500 > OSP_{60}- 2500> OSN-1850.

V_{mic} were: OSN-1850 > OSP_{70}- 2500 > OSP_{80}- 2500 > OSP_{60}- 2500.

V_{meso} were: OSP_{60}- 2500> OSP_{80}- 2500> OSP_{70}- 2500> OSN-1850.

From the economic or commercial application point of view, the sample OSP_{80}- 2500 prepared from olive stone, cheap and available precursor, has the advantages: micro- and meso-porosity; high surface area 2050 m^2/g, high bulk density 0.833 g/ml and total pore volume,

V_p, 1.0836 ml/g which is comparable for activated carbons in markets. Therefore, it is useful in wide applications in wastewater treatment plants, not only for purification of drinking water.

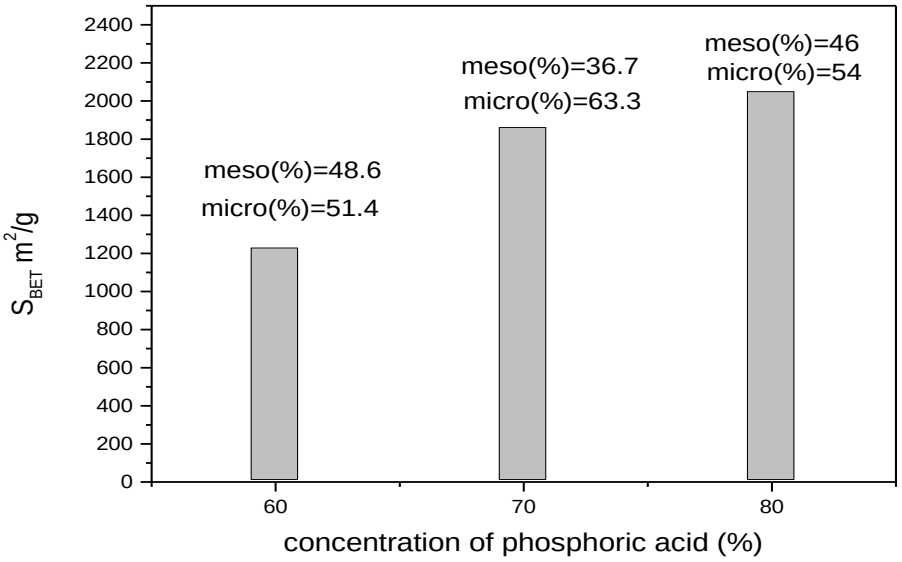

Fig. (3.2) The relation between concentration of H_3PO_4 (%) and surface area of activated carbons.

.

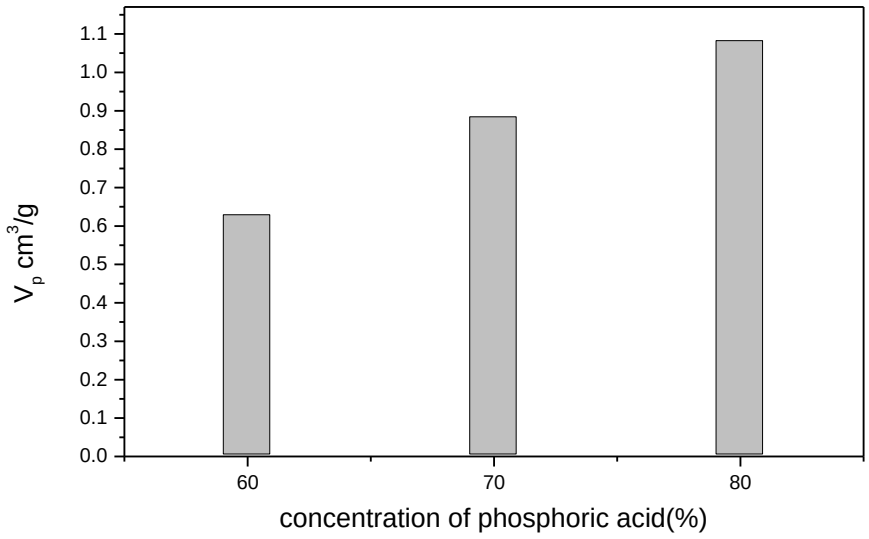

Fig. (3.3) The relation between concentration of H_3PO_4 (%) and total pore volume (V_p) of activated carbons.

3.2.5. Scanning Electron Microscope

The scanning electron microscopy images gave insight into the olive stone structure with respect to its shape. The dark areas are macro pores and the pale grey areas are due to the carbon matrix.

Figs.(3.4) represent the morphology of the resulting activated carbon prepared via physical and chemical activation methods, respectively. It can be clearly seen that physical and chemical activations show some changes in the surface of the particles after activation. The different pore structures of the activated carbon prepared from either physical (using nitrogen as activating agent) or chemical (using H_3PO_4) activation are observed, which depend upon different reaction mechanisms. Fig (3.4) depicts three magnifications: 1600 x; 800x and 50x. For comparison between chemical and physical activations, same magnification 1600x may be useful. In this concern, the sample OSN-1850 activated by N_2 gas indicated that the carbon matrix are greater than the dark areas. This is referred to the nature of the micro pores resultant from the activated N_2 gas. Whereas, the dark areas are greater than the carbon matrix using H_3PO_4 as activated in chemical activation. This implies to the higher surface area of sample OSP_{70}-2500 due to meso-pores as well as to micro-pores.

Also, this shows that the olive stone activated by H_3PO_4 have irregular carbon matrix. i.e., of different shapes and sizes. This was proved by nitrogen adsorption isotherms of activated olive stone

which indicated that they were mainly micro pores only in physical activation and mixture from micro- and meso pores in chemical activation.

This may be explained by progressive changes in the surface of the cellular structure of the parent material with H_3PO_4 solution used as shown in Fig (3.4). The cellulose units are hydrolyzed by the acid and thus the main components of the inter cellular wall are broken down to smaller structure. Thus, it is apparent that the external surface of olive stone is quite rough, consisting of cavities, cracks, and irregular protrusions.

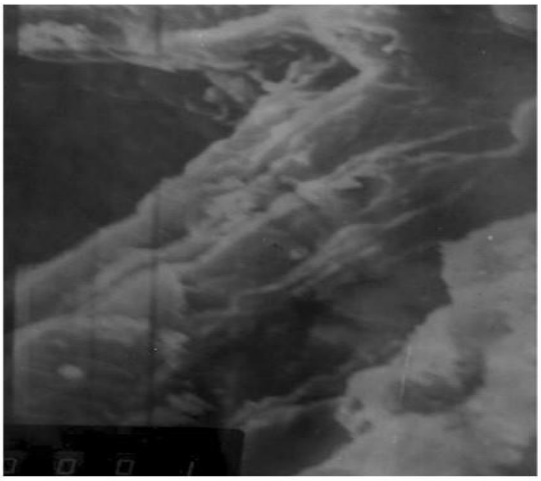

OS P70 – 2500(1600x)

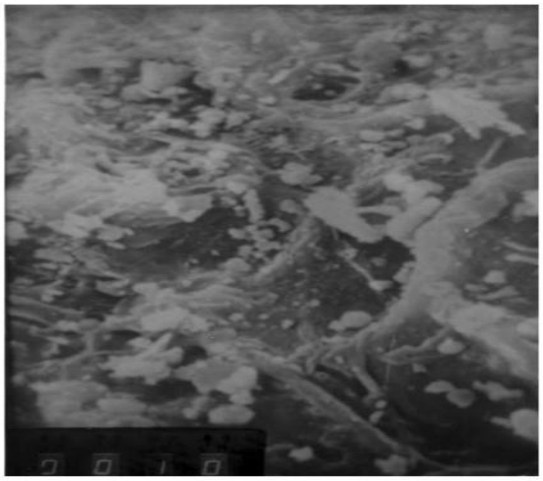

OS N – 1850(1600x)

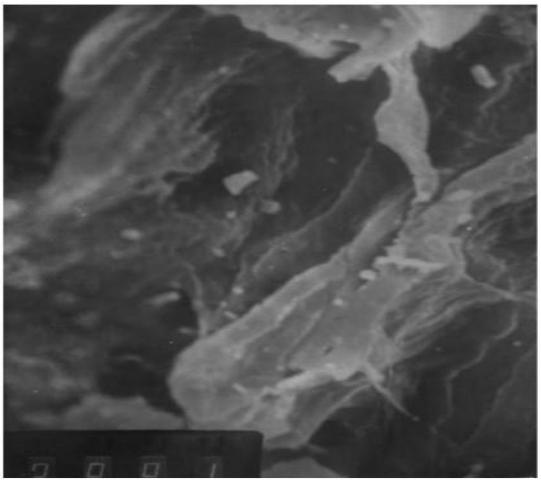

OS P80 – 2500(800x)

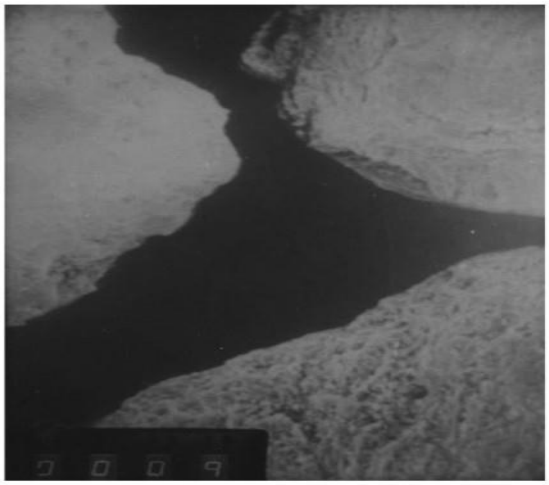

OS P60 – 2500(50x)

Fig (3.4) Scanning Electron microscope (SEM) of prepared carbons

3.3. Adsorption Experiments:

3.3.1. Selection of active carbons

Table (3.4) shows the results of the initial laboratory tests for removal of THMs. The results of adsorption experiments are presented either by uptake (µg/g) or percent removal (Re%) and indicated that activated carbon prepared by H_3PO_4 is better than N_2 gas in removal of trihalomethanes (THMs). In this concern, sample OSP_{60}-2500 is suitable to remove boromoform ($CHBr_3$) whereas sample OS P_{80} -2500 is suitable to remove either chloroform ($CHCl_3$) or dibromochloromethane ($CHBr_2Cl$) and sample OSP_{70}-2500 is suitable to remove dichlorobromomethane ($CHBrCl_2$). Consequently, four adsorption systems were chosen for further investigations. These are: OSP_{60}-2500 : $CHBr_3$; OSP_{80} -2500 : $CHCl_3$; OSP_{80} -2500 : $CHBr_2Cl$ and OSP_{70}-2500: $CHBrCl_2$.

Table (3.4) Adsorbability of THMs using the prepared activated carbons

Compound	Adsorbability							
	OSN – 1850		OS P_{60} – 2500		OS P_{70} –2500		OS P_{80} – 2500	
	Re%	Uptake (µg/g)	Re%	Uptake (µg/g)	Re%	Uptake (µg/g)	Re%	Uptake (µg/g)
Chloroform	9	5.9	18.3	27.5	37.8	56.7	46.6	69.9
Dichloroboromomethane	10	14.8	38.3	57.5	58	87.5	40.3	60
Boromoform	8.5	13.4	58	78	45	25	16.9	75.1
Diboromochloromethane	33.7	50.6	50.2	81.2	37	56.2	59.2	89.4

3.3.2. Factors Affecting Adsorption Process

3.3.2.1. Effect of agitation time

The kinetic investigations on the adsorption of THMs using (OSP_{80} -2500 , OSP_{60} -2500 and OSP_{70} -2500) carbons are given in Fig.(3.5). As agitation time increased, the THMs removal also increases initially, but then gradually approaches a constant value, denoting attainment of an equilibrium. Obviously, the equilibrium was attained after shaking for about 1750 min in case of boromoform and shaking for about 1200 min in case of chloroform , shaking for about 600 min in case of diboromochloromethane , shaking for about 1200 min in case of dichloroboromomethane , beyond which there is no further increase in the adsorption.

The curves shown in Fig.(3.5), present a double nature, the removal of each THMs is high in the initial time, but there after the rate significantly levels off and eventually zero, i.e. equilibrium is attained. These changes in the rate of removal may be due to the fact that, initially adsorption sites were vacant and the solute concentration gradient was high. Afterwards, the THMs uptake rate by the adsorbent decreases significantly, due to decrease in adsorption sites. In other words, adsorbed THMs firstly occupy highest-energy sites at low surface coverage. As the high-energy sites become saturated, THMs progressively occupy lower-energy sites, resulting in the decrease of the average binding energy on the surface. It is also clear that bromoform has the maximum adsorption capacity followed by

chloroform then dichlorobormomethane then diboromochloromethane Concerning (OSP_{80} -2500 , OSP_{60} -2500 and OSP_{70} -2500) carbon curve in Fig.(3.5) this behavior could be explained on the basis that the longer contact time to reach equilibrium for lower initial THMs concentration may be explained by the fact that diffusion mechanisms control the adsorption of THMs onto olive stone activated carbon . the order of adsorption was found to be $CHCl_3$ >$CHBrCl_2$>$CHBr_2Cl$ >$CHBr_3$. This may be attributed to the fact that adsorption occurs with molecules that are small enough in size to enter the inner cavities through the pores. Therefore, the adsorption rate increases with decreasing size of the adsorbed molecules [104].

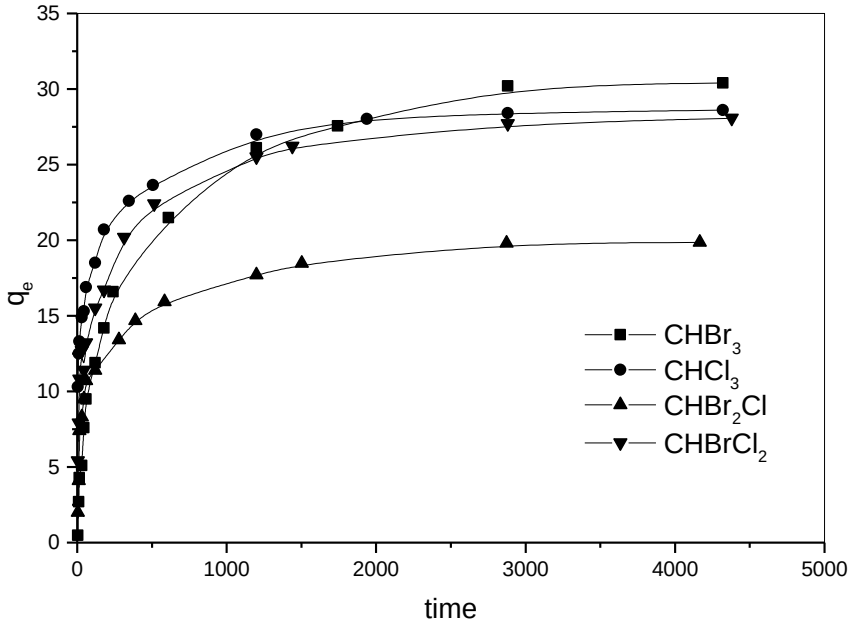

Fig (3.5) Effect of agitation time on the adsorption of THMs. Experimental conditions employed: (V) = 5 ml ; (m) = 0.01 g ; (C_o) = 100 µg/L

3.3.2.2. Kinetic parameters

The kinetic experimental data of adsorption of THMs onto activated carbons are simulated by pseudo-first-order and the second-order rate equations to analyze the adsorption kinetics of the 4 adsorption systems: OS P_{60}-2500 : $CHBr_3$; OS P_{80} -2500 : $CHCl_3$; OS P_{80} -2500 : $CHBr_2Cl$ and OS P_{70}-2500: $CHBrCl_2$.

$$\text{(Pseudo – first – order)} \qquad \log(q_e - q_t) = \log q_e - \frac{k_1}{2.303} t$$

$$\text{(Pseudo-second – order)} \qquad \frac{t}{q_t} = \frac{1}{k_2 q_e^2} + \frac{t}{q_e}$$

Where q_e and q_t are amounts adsorbed (µg/g) at equilibrium and t time (min), respectively. k_1 and k_2 are the adsorption rate constants of pseudo-first-order (min^{-1}) and pseudo second-order (g/mg min.) respectively. The results are showed in Figs. (3.6 and 3.7).

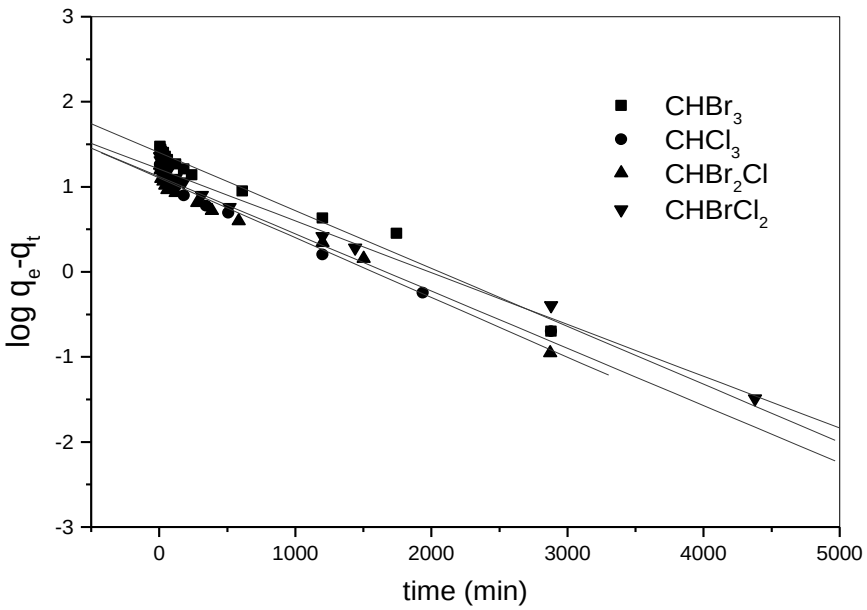

Fig(3.6) The pseudo-first-order adsorption kinetics of THMs .

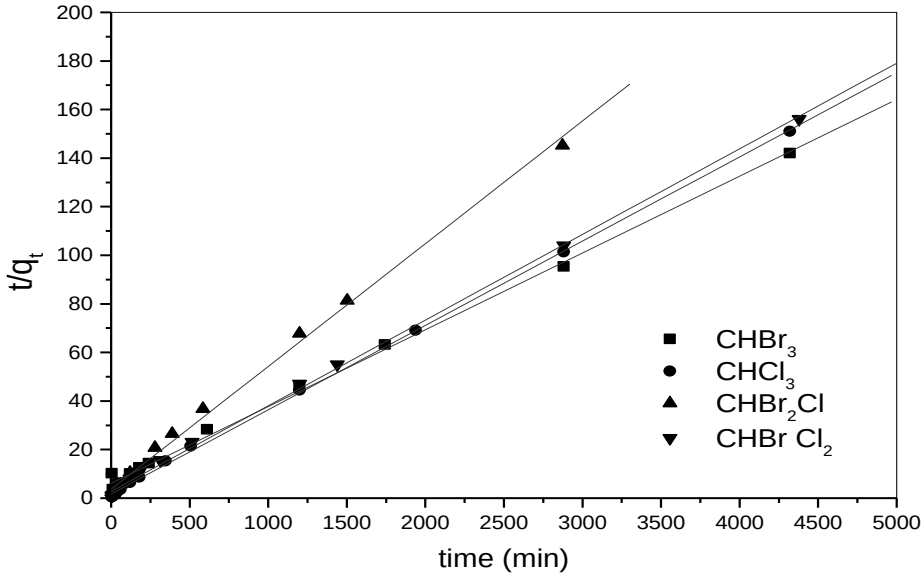

Fig (3.7) The pseudo-second-order adsorption kinetics of THMs .

Remarkably, the kinetic data of the chloroform, boromoform, diboromochloromethane , dichloroboromomethane may be described well by second-order rate equation due to the high values of correlation coefficient R^2 for second-order adsorption model compared to that of pseudo-first-order model. The calculated equilibrium adsorption capacities $q_{e,cal}$ from second-order model agree well with the experimental values. These results suggest that the sorption system is not first-order reaction and that the second-order model, based on the assumption that the rate-limiting step may be chemical sorption involving valency forces through sharing or exchange of electrons between THMs and adsorbent [105-107].

The initial adsorption rate (h) determined by the second-order rate equation are listed in Table (3.5). The values of the adsorption rate constant for chloroform, boromoform , diboromochloromethane , dichloroboromomethane are 0.15 , 0.13 , 0.092 and 0.0712

respectively. These results confirm the data obtained by maximum adsorption capacity from equilibrium time curves.

Table (3.5) Kinetic parameters on the adsorption of THM

	$CHBr_3$	$CHCl_3$	$CHBr_2Cl$	$CHBrCl_2$
Q_e (exp) (µg/g)	30.4	28.6	19.8	28
Pseudo-first-order equation				
Q_e (µg/g)	25.1	12.5	12.5	15.8
k_1 (min^{-1})	15.6	15.4	16.1	13.8
R^2	0.984	0.975	0.978	0.981
Pseudo-second-order equation				
Q_e (µg/g)	33.3	33.6	20	33.3
k_2 ($\times 10^{-4}$ g/mg min)	1.47	5.3	6.7	3.3
h (mg/g min)	0.15	0.13	0.092	0.0712
R^2	0.999	0.999	0.999	0.999
Intraparticle diffusion equation				
k_{int} (mg/g $min^{0.5}$)	0.58	0.51	0.2	0.6
C	6.5	12.7	8.7	8.5
R^2	0.976	0.958	0.979	0.989

3. 3. 2.3. **Diffusion Studies.**

From a mechanistic viewpoint to interpret the experimental data, prediction of the rate-limiting step is an important factor to be considered in the sorption process [108]. In order to show the existence of intra-particle diffusion in the adsorption process, results were subjected to the Weber-Morris according to the following equation.

$$q_t = k_{int}\, t^{0.5}$$

where q_t is the amounts adsorbed (μg/g) at time t and k_{int} is the intra-particle diffusion rate. The intra-particle diffusion rates were determined from the plots of q_t versus $t^{0.5}$ as shown in Fig.(3.8). If intra- particle diffusion is a rate-controlling step, then the plots should be linear and pass through the origin. As can be seen, the plots have the same general features. They have an initial curved portion, followed by an intermediate linear portion, and a plateau. The initial portion of these plots is due to external mass transfer, the intermediate linear part is due to intra-particle diffusion, and the plateau is due to the equilibrium stage where intra-particle diffusion starts to slow down due to extremely low solute concentrations in the solution [109,110].

The slope of linear portion has been defined as intra-particle diffusion rate parameter k_{int}. The k_{int} were determined and listed in Table (3.5) and their values are: 0. 58, 0.51, 0.2 and 0.6 $mg.g^{-1}min^{-0.5}$

for bromoform; chloroform; dibromochloromethane and dichlorobromomethane, respectively.

On the other hand, the intercept of the plot reflects the boundary layer effect. The larger the intercept, the greater is the contribution of the surface sorption in the rate-limiting step [111,112], and it follows the sequence:

Chloroform < dichlorobromomethane < dibromochloromethan < bromoform

suggesting less contribution of surface sorption in case of $CHCl_3$ than $CHBrCl_2$ less than $CHBr_2Cl$ than $CHBr_3$.

Ho, [113] has shown that it is essential for the q_t vs. $t^{0.5}$ plots to go through the origin if the intra-particle diffusion is the sole rate-limiting step [113]. Since this was also not the case in the present work, the q_t vs. $t^{0.5}$ plots have intercept, it may be concluded that the intra-particle diffusion was not the only rate-controlling step. The sorption mechanism of THMs from aqueous solution is rather complex process, probably a combination of external mass transfer, and intra-particle diffusion which contribute to the rate determining step **[114]**. This behavior is predicted when a large initial fraction of the reaction is controlled by intra-particle diffusion.

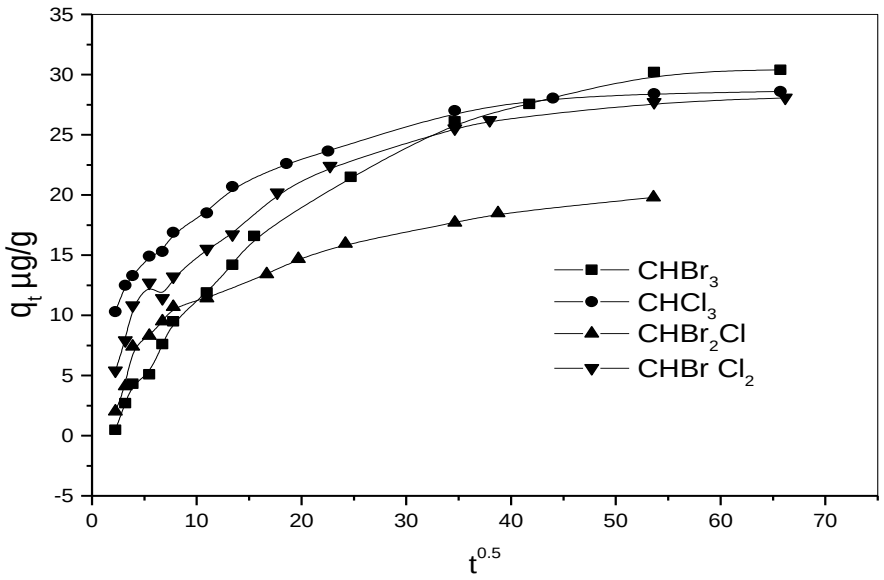

Fig (3.8) The intra-particle diffusion Plots for THMs adsorption.

3.3.2.4. Effect of initial concentration of THMs.

The effect of the initial adsorbate concentration on the removal of THMs by activated carbons was studied over an initial THMs concentration range of 10-300 µg/L . Fig (3.9) shows that, as adsorbate concentration increases, the adsorbed amount increases too. Increasing the initial concentration provides an important driving force to overcome all mass transfer resistance of each THM between the aqueous and solid phase and accelerates the diffusion of THMs from solution onto adsorbents[(115)], which would result in higher adsorption. However, the increase in each initial THM adsorbate concentration beyond about 100 µg/L causes little increase in the amount adsorbed for each indicating that the adsorption sites are saturated. At different initial concentrations of THMs for a fixed adsorbent mass, the surface sites are fully exposed. With increased

concentration there is an increase in adsorption capacity up to a certain values, which may be due to a high intarmolecular competitiveness to occupy the lower energetic surface sites left behind. After saturation point the process becomes purely reversible and there will be no adsorption [116].These results may be explained considering that, at low adsorbate concentration, the ratio of surface active sites to THMs concentration is high, hence the THMs could interact with the sorbent to occupy the active sites on the carbon surface sufficiently and be removed from the solution [115]. But with the increase in adsorbate concentration, the number of active adsorption sites is not enough to accommodate THMs

On a relative basis, however, the percentage removal (Re%) was greater at lower initial concentration and smaller at higher initial concentrations (Fig. 3.9). In diluted solutions, the mobility of THMs is high, probably for this reason, the interaction of these compounds with the adsorbent was increased[117] by increasing THMs concentration.

These results clearly indicate that the removal of THMs from the aqueous solution was dependent on the concentration of THMs present in the system. At low concentration (below 100 µg/L for THM) sorption was 85-95%. This suggests that olive stone activated by H_3PO_4 is suitable to remove most of THMs exist as DBPs in drinking water. Thus, concentration of THMs reaches the permissible

levels according to the standard regulations. Consequently, the drinking water will be safe without any health risk.

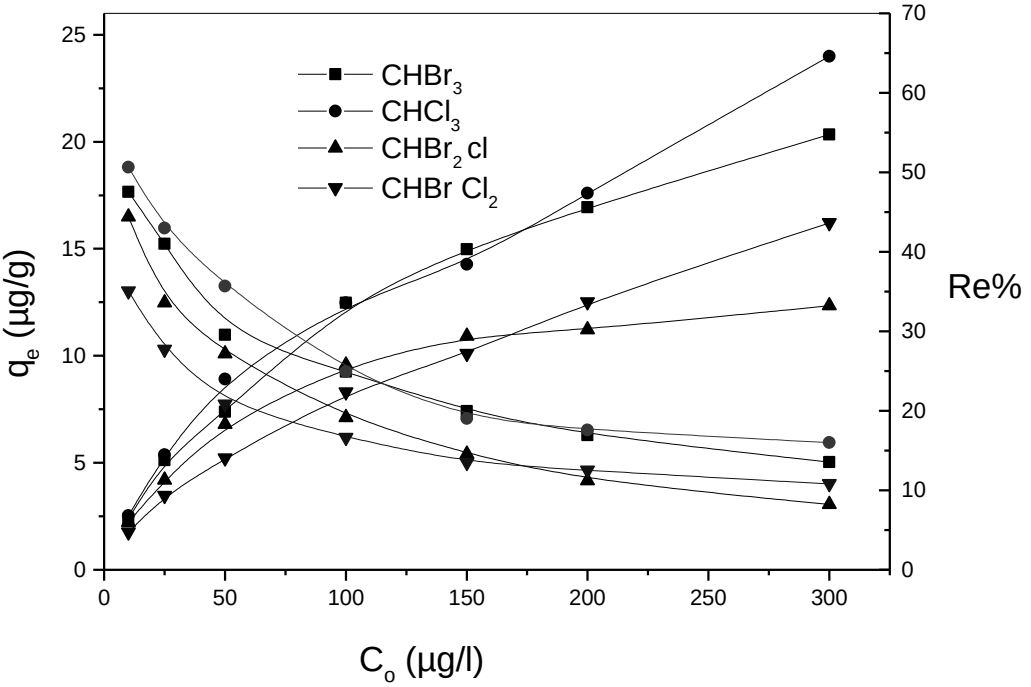

Fig (3.9) Effect of initial concentration of THMs on adsorption. Experimental conditions employed: (V) = 5 ml; (m) = 0.02 g and ; initial THMs conc. (C_o) = 10-300 µg/L

3.3.2.5. Effect of adsorbent mass on adsorption

Fig. (3.10) shows the effect of adsorbent dosage on the corresponding adsorption capacities, q_e, and percentage removal Re%, of THMs from aqueous solution onto olive stone activated carbons. Increasing the adsorbent concentration led to an increase in the percentage removal of THMs (Re%) but to a decrease in the adsorption capacity (q_e). It was clear that each compound has the same pattern. In this concern, as the adsorbent dosage increases the percent removal (Re%) of each THMs increases too. This is occurred

from 5 ml solution containing 100 µg/L of chloroform or boromoform or diboromochloromethane or dichloroboromomethane and then attained constant removal after a particular carbon concentration (optimum dosage) beyond which there is no significant increase in removal for THMs studied.

There are many factors, which can contribute to this adsorbent concentration effect, the first and most important factor is that as (i) the dosage of adsorbent is increased, the adsorption sites remain unsaturated during the adsorption reaction leading to drop in adsorption capacity (q_e). (ii) On the other hand, an increased number of available adsorption sites increase in the adsorbent dose are able to adsorb more . THMs thus resulting in an overall increase in the percent removal (Re%) [118]. (iii) The aggregation/agglomeration of sorbent particles at higher concentrations, which would lead to a decrease in the surface area and an increase in the diffusional path length. The particle interaction at higher adsorbent concentration may also help to desorbs some of the loosely bound THMs from the sorbent surface[119]. As a result, the removal of a given amount of solute can be accomplished with greater economy of adsorbent if the solution is treated with separate small batches of adsorbent rather than in a single batch, with filtration between each stage [120]. (iv) The decreases of loading capacity q_e with the increase in the adsorbent dose is consistent with the argument that surface sites of carbon are heterogeneous. According to the surface site heterogeneity model, the surface is composed of sites with a

spectrum of binding energies. At low adsorbent dose, all types of sites are entirely exposed for adsorption and the surface gets saturated faster. But at higher particle concentrations, there is larger fraction of higher energy sites becoming unoccupied. So the active adsorption sites are more at a fixed adsorbate concentration with no saturation [121].

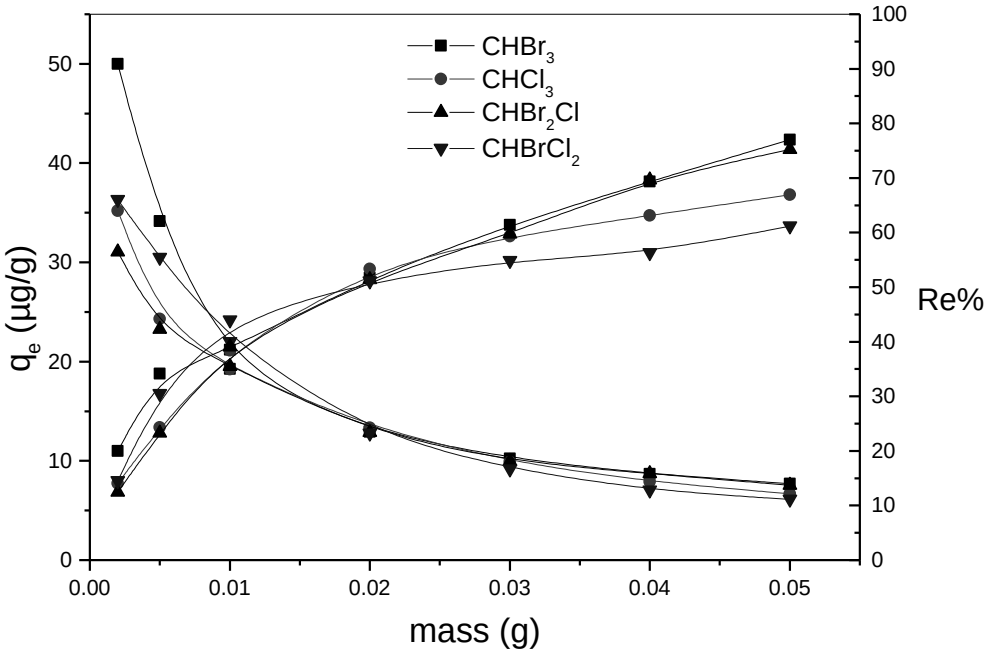

Fig (3.10) Effect of adsorbent mass on adsorption of THMs. Experimental conditions employed: (V) = 5 ml; (m) = 0.01 - 0.05 g; conc. (C_o) = 100 µg/L

3.3.2. 6. Effect of pH value

Fig. (3.11) shows the effect of pH range (1.3-8) on adsorption of chloroform or Bromoform or diboromochloromethane or dichloroboromomethane onto olive stone activated carbons with initial concentration of 100 µg/L. It is obvious that the adsorption of THMs removal followed the same pattern for all the compounds.

This may be due to the fact that the employed olive stone activated carbon have been purified by acid solution to improve their properties which may enhance the resistance of olive stone activated carbon to acid environment. However, the adsorption of each THMs decreases as the pH increased. This is due to the fact that more oxygen-containing groups on the olive stone activated carbon surface are ionized at higher pH values and thus they adsorbed more water [(122)]. The formation of water clusters on these groups would block the access of THMs molecules to the adsorption sites and lead to a smaller adsorption of THMs.

Second, there are many oxygen-containing groups attached on the surface of purified olive stone activated carbon, which made olive stone activated carbon become more hydrophilic and suitable for adsorption of relatively polar molecules [(123)] .

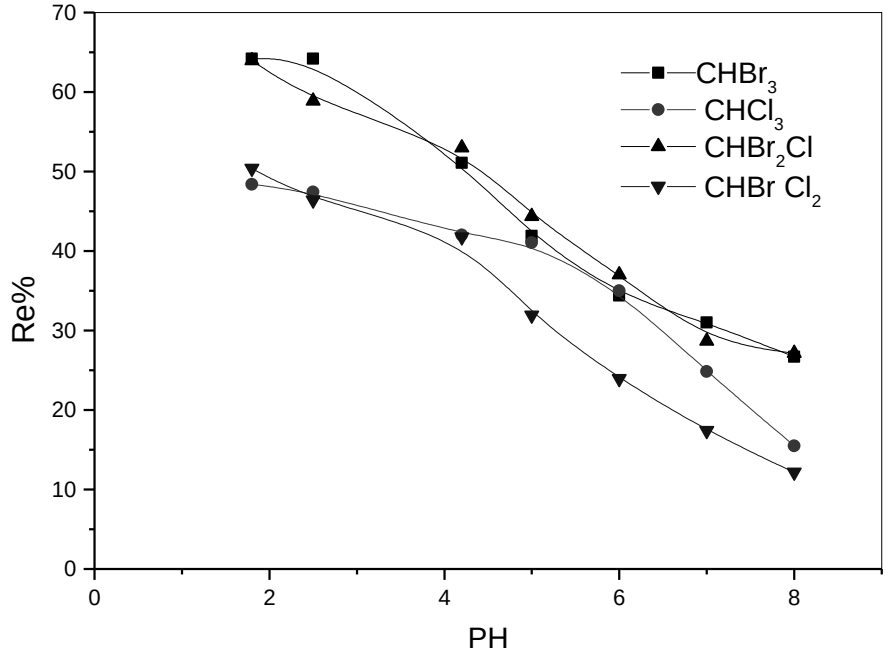

Fig (3.11). Effect of pH on the adsorption of THMs . Experimental conditions employed: (V) = 5 ml; (m) = 0.01 g ; (C_o) = 100 µg/L.

3.3.2.7. Equilibrium Adsorption Isotherms of THMs

Adsorption data for wide range of adsorbate concentrations are most conveniently described by adsorption isotherm, which relate adsorption density q_e (metal uptake per unit weight of adsorbent) to equilibrium adsorbate concentration in the bulk fluid phase, C_e. The adsorption isotherms of chloroform , boromoform, diboromochloromethane or dichloroboromomethane were obtained in an attempt to get a more thorough insight to the adsorption mechanism and maximum adsorption capacity of each compound onto activated carbons .

In this concern, the experimental results obtained for the adsorption of chloroform and diboromochloromethane onto sample OS P_{80} -2500; boromoform onto OS P_{60} -2500 and dichlorobormomethane onto OSP_{70} -2500 carbon at room temperature (25±1 ^{o}C) under optimum conditions of contact time and pH were given in Fig. (3.12). Initially the isotherms raise rapidly over the initial stage of adsorption where low C_e and q_e values existed. This behavior indicates that there were plenty of readily accessible sites available on the used adsorbents. Eventually a slow approach to equilibrium at high concentrations occurred. As more sites are filled, it becomes more difficult for the solute molecules to find a vacant site available for adsorption and/or the difficulty of molecules in penetrating the adsorbed layer already covering the surface sites. As result, the rate of adsorption decreases giving a plateau covers a wide range of solution concentration. i.e. considerably increasing the C_e values for a small increase in q_e.

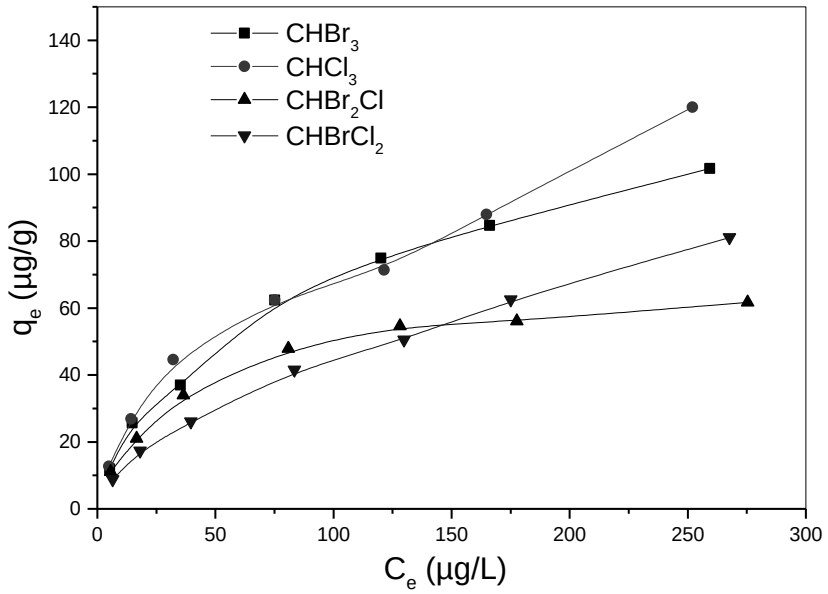

Fig (3.12) Equilibrium adsorption isotherms of THMs .

3.3.2.8. Isotherms modeling

Adsorption isotherm describe how adsorbates interact with adsorbents and are critical in optimizing the use of adsorbents. To optimize the design of a sorption system to remove THMs from effluents, it is important to establish the most appropriate correlation for the equilibrium curves. The experimental data of equilibrium isotherms for the 4-adsorption systems OSP_{60}-2500 : $CHBr_3$; OSP_{80} -2500 : $CHCl_3$; OSP_{80} -2500 : $CHBr_2Cl$ and OSP_{70}-2500: $CHBrCl_2$ were modeled for further investigations using the most frequently used isotherms: Langmuir and Freundlich, [124].

The parameters of all two models can be obtained from slopes and intercepts of the following equations:

$$\log q_e = \log K + \frac{1}{n} \log C_e$$

$$\frac{C_e}{q_e} = \frac{1}{bq^o} + \frac{C_e}{q^o}$$

Where q_e is the equilibrium uptake (µg/g)

C_e the equilibrium concentration (µg/L); and

K and n are the Freundlich constants, n gives an indication of favorability (adsorption intensity) and k the capacity of adsorbent (adsorption capacity).

The isotherm parameters are given in Table (3.6). The applicability of the isotherm equation is compared by judging the non-linear correlation coefficients R^2. In a view of value of non-linear R^2, Langmuir isotherm gives good fit ($R^2 > 0.99$) for THMs.

(A) Langmuir Model

Fig.(3.13) shows linear relationship of C_e against C_e/q_e indicating the applicability of Langmuir model. Table (3.6) shows that the Langmuir constants 'b' which reflect the binding strength between sorbent and sorbate, are different for THMs. In this concern, the b-value is more for dibromochloromethane onto sample OS P_{80}-2500 than for bromoform onto sample OS P_{60}-2500; chloroform onto sample OS P_{80}-2500; dichlorobromomethane onto sample OS P_{70}-2500 , thereby indicating strong bonding of dibromochloromethane with carbon surface in comparison to other THMs. i.e. the THMs exhibit different sorption characteristics i.e., some are strongly adsorbed e.g. dibromochloromethane and bromoform , whereas the weakly adsorbed is dichlorobromomethane .

According to the Langmuir equation, q^o is the limiting amount of adsorbed compound required to give a complete monolayer on the carbon and b, is a measure of the relative adsorption affinity. From Table (3.6), the adsorption capacity or the monolayer coverage determined by Langmuir isotherm follows the order : $CHCl_3 > CHBr_3 > CHBrCl_2 > CHBr_2Cl$ whereas adsorption affinity, b, sequence trend obtained in the present work was $CHBr_2Cl > CHBr_3 > CHCl_3 > CHBrCl_2$. It is worth to mention that the adsorptive capacity does not follow the same order as the adsorption affinity. This is logic considering that q^o values depend on the solute concentration and the adsorbent mass while the coefficients $b \alpha e^{-\Delta H/RT}$ where the driving force is the enthalpy change, ΔH.

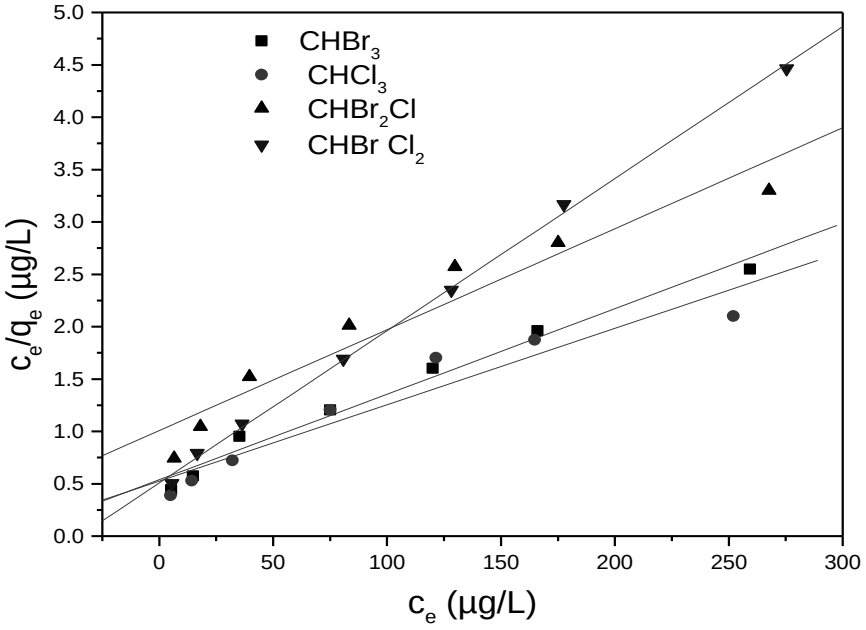

Fig. (3.13). Langmuir plots of THMs adsorption

(B) Freundlich Model

Fig. (3.14) shows satisfactory linear relationship of log C_e against log q_e indicating also the applicability of the Freundlich model. Accordingly, Freundlich isotherm parameters (K, n) for boromoform, chloroform, diboromochloromethane and dichloroboromomethane are summarized in Table (3.6). The constant K represents the capacity of each sorbent OSP_{80} -2500 , OSP_{60} -2500 and OSP_{70} -2500 for the solute under investigations while the constant n represents the strength of the adsorption of the solute by adsorbent. Together, K and n determined the shape of the isotherm.

In general, an isotherm shows that one component adsorbs more than another if it has a higher value of K at the same

equilibrium concentration, if its data have a lower slope, and if its equilibrium points extend to a lower value of equilibrium concentration. In our study this rule is applicable for $CHCl_3$ which have higher K and lower slope than that of other THMs. From Table (3.6), the values of 1/n were found in the range 0.45 to 0.58, i.e., i The values of the Freundlich exponent " n " are greater than one, indicating that the adsorption of chloroform , boromoform, diboromochloromethane, dichloroboromomethane by carbon OS P_{80} -2500 , OSP_{60} -2500 and OSP_{70} -2500 is favorable[125]. indicating that surface structures of sorbents (OSP_{80} -2500 , OSP_{60} -2500 and OSP_{70} -2500) are heterogenous[126]. However, it is clear that adsorption of chloroform and diboromchloromethane is more favorable than the boromoform then dichlorobormomethane as indicated higher capacity at the same equilibrium concentration and higher intensity.

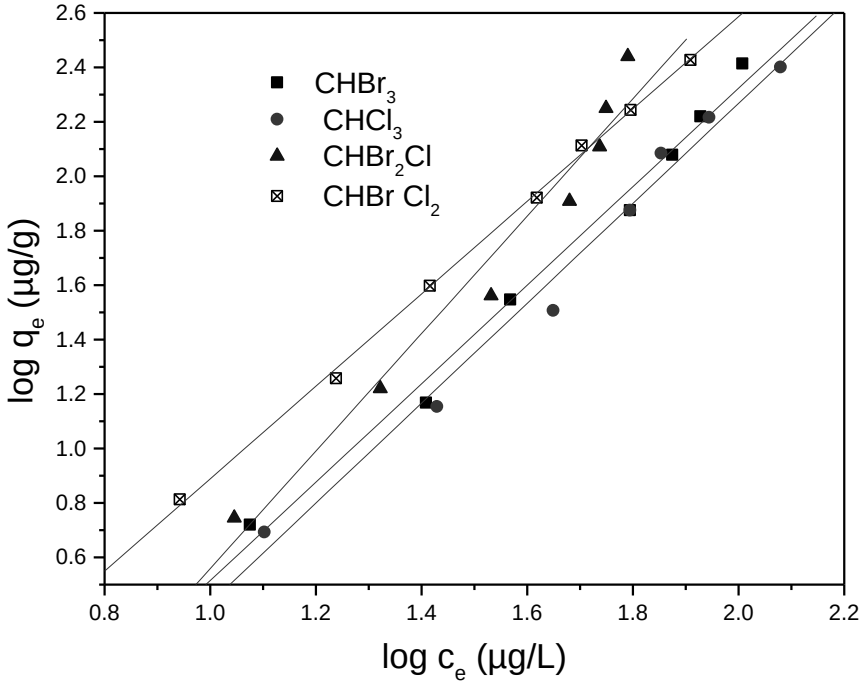

Fig. (3.14) Freundlich plots of THMs adsorption.

Table (3.6) Langmuir and Freundlich parameters of THMs adsorption

	Frundlich				Langmuir		
Sorbate	K(µg/g)	1/n	n	R^2	q^o (µg/g)	b (ℓ/mg)	R^2
$CHBr_3$	5.2	0.55	1.8	0.998	125	0.015	0.999
$CHCl_3$	5.8	0.58	1.7	0.999	142.8	0.014	0.956
$CHBr_2Cl$	5.8	0.45	2.2	0.988	71.4	0.02	0.998
$CHBrCl_2$	2.4	0.50	2.0	0.998	111.1	9×10^{-3}	0.937

3.3.2.9. Temperature Effect

Variations in temperature cause adsorbent rearrangements and also Changes in the adsorption/ desorption equilibrium. The uptake of bromoform onto OSP_{60}- 2500 and chloroform onto OSP_{80}- 2500 at 25°C, 35°C and 45°C are presented in Fig (3.15) and (3.16) respectively. It is clear that both adsorption systems indicate a normal trend associated with physical adsorption. In this concern, an increase in the temperature, will result in a reduction of the equilibrium adsorptive capacity, whereas lower temperature will favor an increased capacity [127].

The decreasing of adsorption capacity of THM with increasing temperature can be referred to the solubility [128] i.e. as the temperature increases, the solubility increases which lead to decreasing of affinity of THM to olive stone activated carbons.

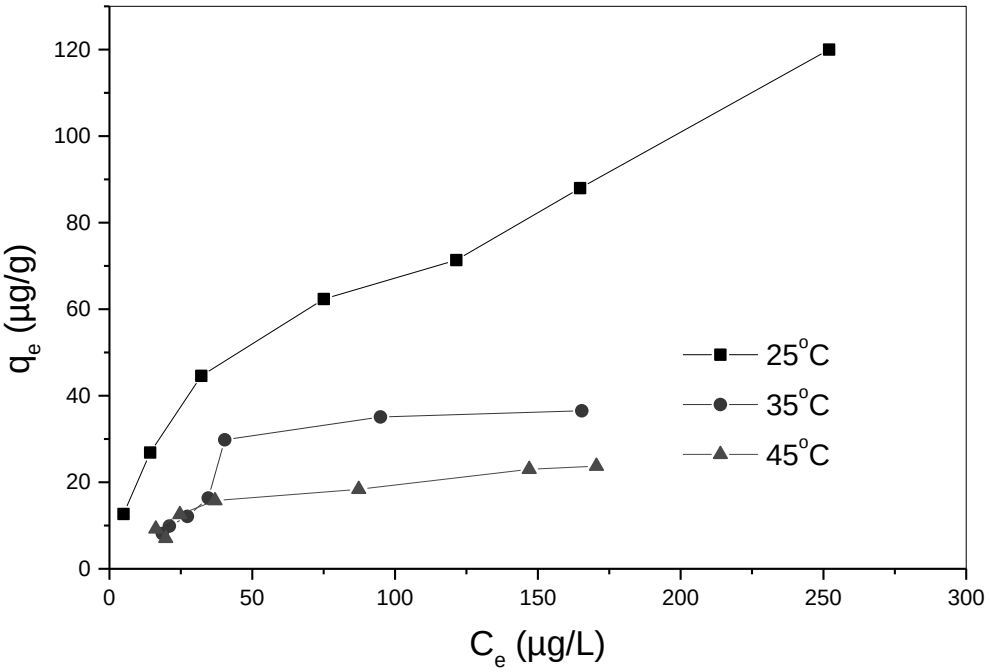

Fig (3.15) Effect of Temperature on adsorption of chloroform. Experimental conditions employed: V = 5 ml; (m) = 0.01 g and initial conc. (C_o) = 100 (µg/L).

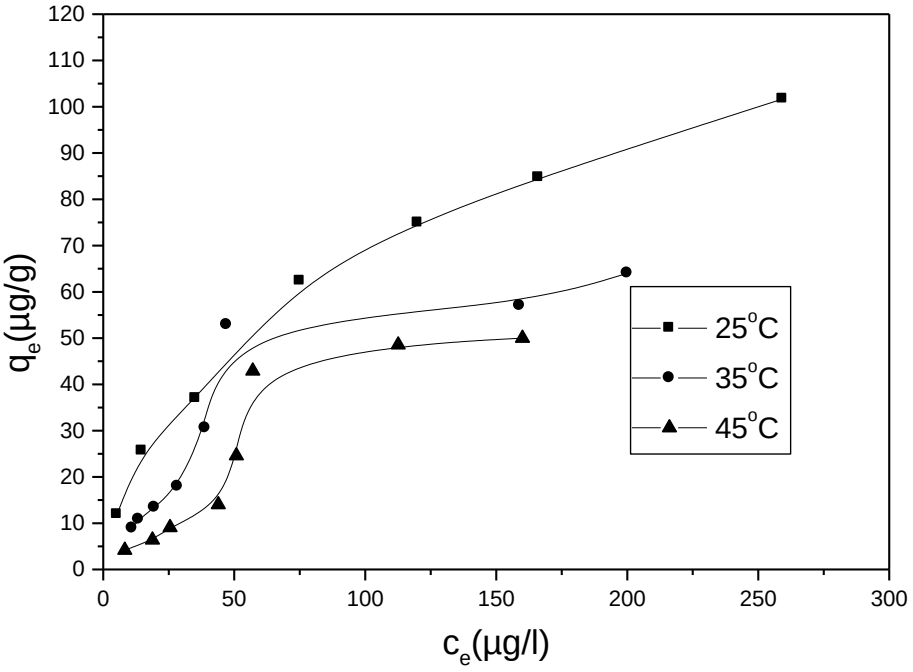

Fig (3.16)Effect of Temp on adsorption of boromoform. Experimental conditions employed: solution THMs: (V) = 5 ml; (m) = 0.01 g and (C_o) = 100(µg/L).

3.4. Photodegradation Studies

Activated carbon is the material most widely used for the adsorption of THMs in water treatment stations due to its high removal capacity, and it has been cited by the U.S. Environmental Protection Agency as one of the foremost materials for use in pollution control[129]. Important studies reviewing the removal of THM and organic molecules by carbon spheres have been published [130]. Nevertheless, the efficiency of activated carbon as an adsorbent is dependent on the need for large dosages over short time periods, with its use being consequently limited by the associated cost. Due to the limitations associated with the above techniques, most researchers have focused on methods of reducing the potential for the formation of THMs, including the use of membrane processes and ultrasonic irradiation [131-134]. Nevertheless, an efficient destructive method for the removal of THMs contaminants from the aqueous environment is still required [135]. One promising method for destroying a wide spectrum of organic compounds is photodegradation, which has been studied extensively for the destructive oxidation of various organic pollutants. This has proved to be very effective, since many organic compounds can be degraded successfully to safer end-products such as CO_2, H_2O and mineral acids [136,137].

However, the literature is still limited concerning the photodegradation of THMs, although the degradation of chlorinated

hydrocarbons with UV light has been investigated [138,139] . One of the limitations of the photodegradation process is the presence of natural organic matter in water. A high loading of suspended matter can cause light scattering effects that diminish the activity of the process [140]. For this reason, integration of the photodegradation process with a physicochemical treatment procedure, i.e. adsorption, appears to be a promising method for overcoming the above-mentioned problems and essential for developing a successful treatment process. The integration of photodegradation and adsorption treatment processes can bring several advantages to wastewater treatment plants. Such a hybrid process would be able to remedy the disadvantages of each technique when operated individually, and hence improve the overall removal efficiency. The objective of the work described in this part was to study the applicability of two environmentally friendly processes, i.e. adsorption and photodegradation, employed either separately or in combination, as a potential water-treatment technology for the removal of THMs on a laboratory scale. The combination of adsorption and UV light methods was hypothesized as resulting in more rapid kinetics than either treatment alone.

In the present work, the photodegradation of the THMs solutions was undertaken by exposing them for 25 min. to (i) UV light alone or (ii) UV light in presence of activated carbon derived from olive stone or (iii) UV light in presence of activated carbon loaded by TiO_2 (see data depicted in Figs. (3.17), (3.18) (3.19) and (3.20). It was observed that, when olive stone activated carbon was added under UV light

illumination, the percentage removal of THMs was greater than in the absence of olive stone activated carbon. The results proved that the percent removal (Re%) for all THMs were more better when TiO_2 impregnated on olive stone activated carbon in presence of UV illumination. TiO_2 was impregnated on various adsorbent supports to increase the surface area of the supported catalysts. Loading TiO_2 on the adsorbent surface increases the probability of photocatalytic oxidation due to: (i) increased adsorption, (ii) support may enhance catalytic activity by introducing acidity to the surface, (iii) increased catalytic efficiency due to TiO_2 polar surface and (iv) reactive intermediate stabilization. This may be explained by the fact that the adsorption rates of THMs (on olive stone activated carbon) and their photodecomposition rates (on UV irradiated olive stone activated carbon/ on UV irradiated olive stone activated carbon Loaded by TiO_2) are influenced by the nature of active sites on the carbon employed. Thus, olive stone activated carbons used in the present studies would appear to play a dual role in both retaining and allowing the photodegradation of THMs and the hydroxyl radicals (HO*) was the primary reactive oxygen species for the photodegradation of THMs[(141)].

All supported catalysts exhibit good photocatalytic efficiency and their performance was always better than that of bare activated carbon or UV alone. The performance improvement can be attributed to the high surface areas of the adsorbent used, crystallinity and particle size of deposited TiO_2[(142)]. Some general conclusions can be

made: (i) All the supported catalysts possess a greater surface area compared to that of bare TiO_2 (50 m^2/g) and (ii) Photocatalytic efficiency of all the supported catalysts indicates the presence of an optimum loading of TiO_2 on the surface.

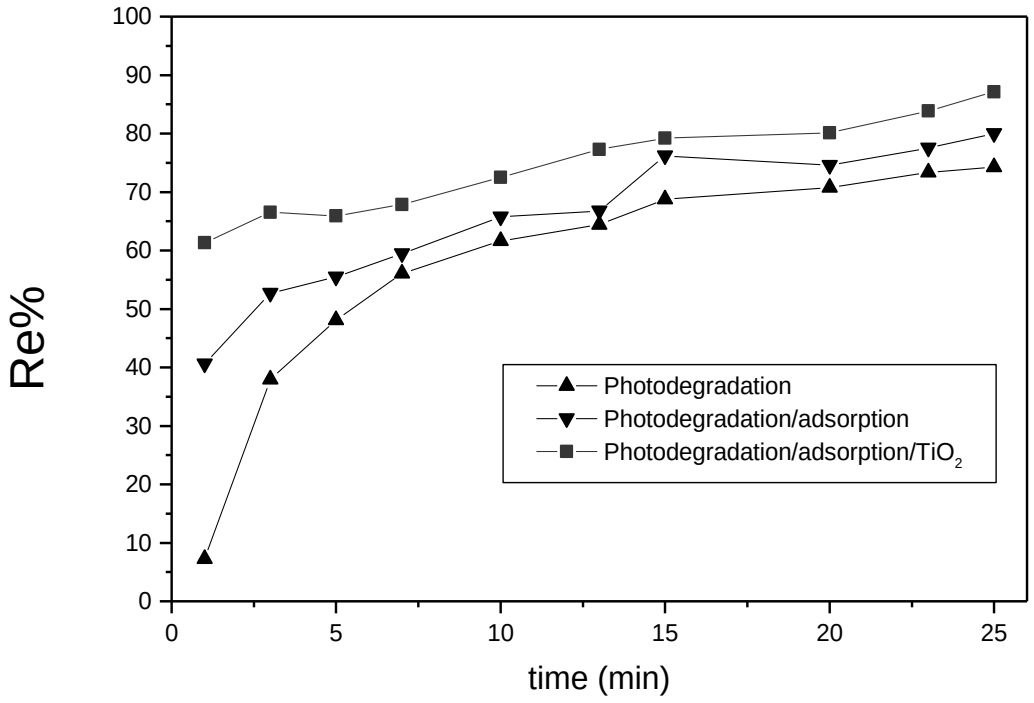

Fig. (3.17) Removal of boromoform from aqueous solution through photodegradation only & photodegradation in the presence of OS P_{60} -2500 and photodegradation in the presence of OS P_{60} -2500 and TiO_2. Data points relate to the following $CHBr_3$. Experimental conditions employed: (V) = 10 ml; (m) = 0.02 g ; initial THMs conc. (C_o) = 100 µg /L

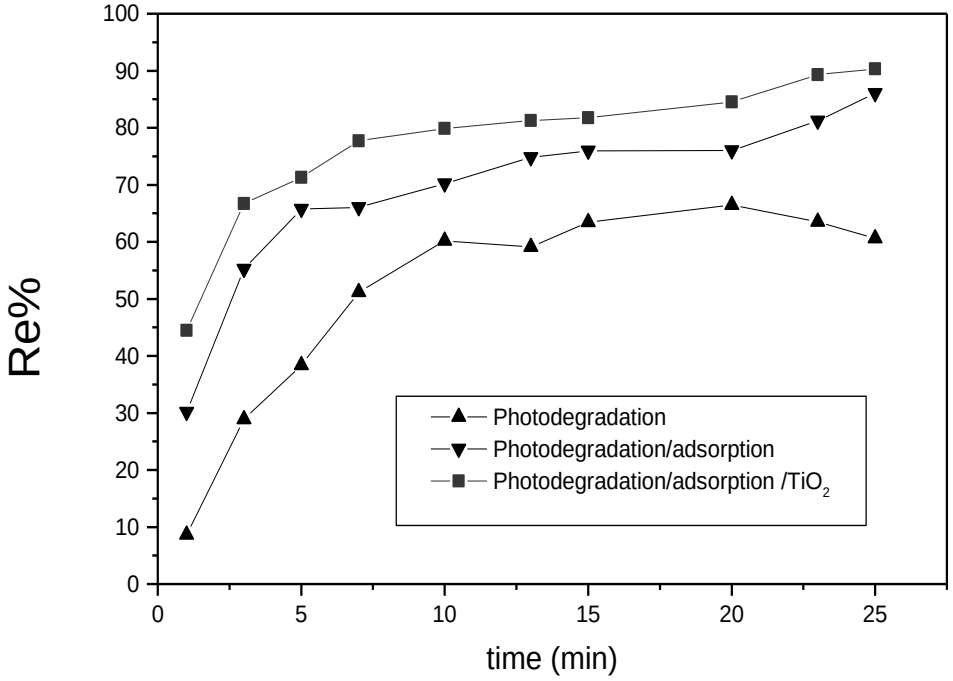

Fig. (3.18) Removal of chloroform from aqueous solution through photodegradation only & photodegradation in the presence of OS P_{80} -2500 and photodegradation in the presence of OS P_{80} -2500 and TiO_2. Data points relate to the following $CHCl_3$. Experimental conditions employed: solution volume (V) = 10 ml; adsorbent mass (m) = 0.02 g; initial THMs conc. (C_o) = 100 µg /L.

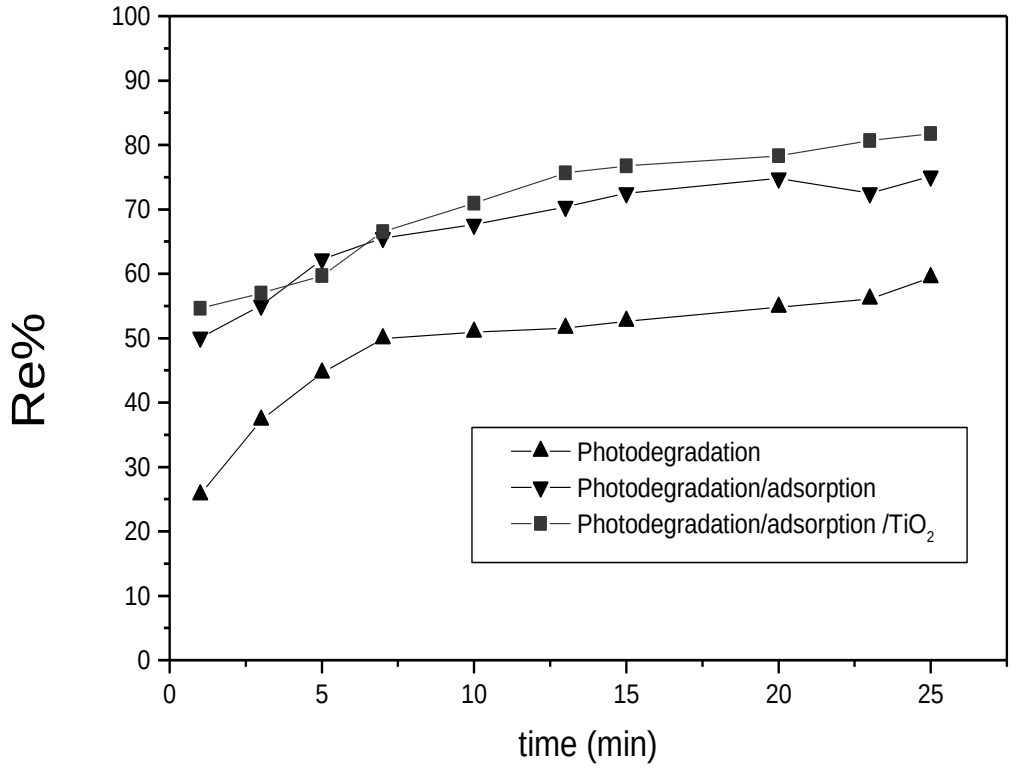

Fig (3.19). Removal of dibormochloromethane from aqueous solution through photodegradation only & photodegradation in the presence of OS P_{70} -2500 and photodegradation in the presence of OS P_{70} -2500 and TiO_2. Data points relate to the following $CHBr_2Cl$. Experimental conditions employed: solutionvolume (V) = 10 ml ; adsorbent mass (m) = 0.02 g; initial THMs conc. (C_o) = 100 µg /L.

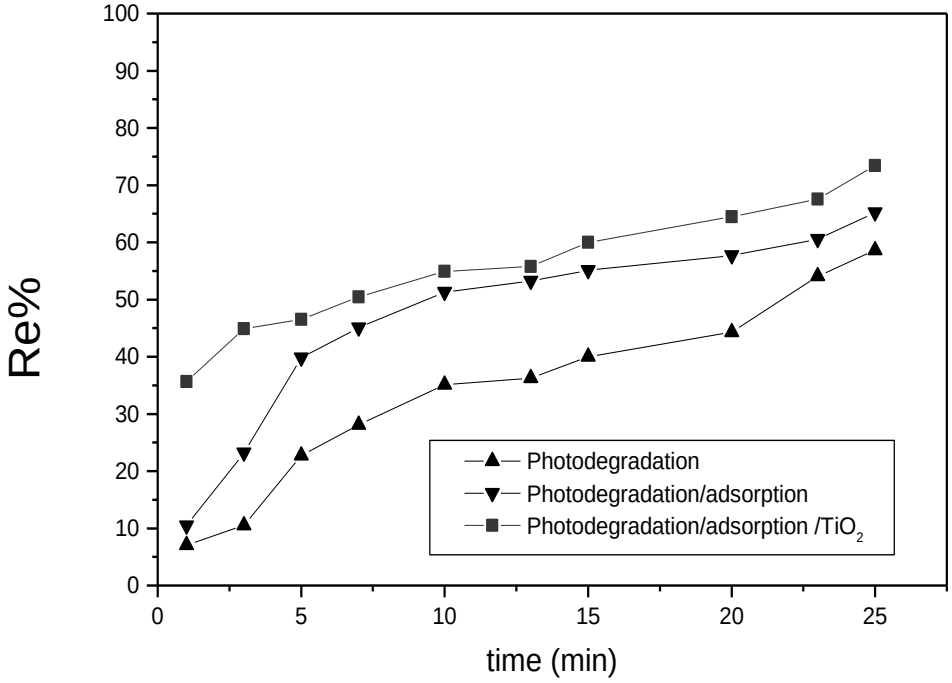

Fig (3.20) Removal of dichlorobormomethane from aqueous solution through photodegradation only & photodegradation in the presence of OS P_{60} -2500 and photodegradation in the presence of OS P_{60} -2500 and TiO_2. Data points relate to the following $CHBrCl_2$. Experimental conditions employed: (V) = 10 ml , (m) = 0.02 g , (C_o) = 100 µg /L.

In order to investigate the photodegradation/adsorption mechanisms involved in the removal of THMs from aqueous solution, the kinetic data were evaluated and described by the Langmuir–Hinshelwood (L–H) pseudo-first-order kinetic model [143].

$$\ln (C/C_o) = - k_{app} t$$

where C is the concentration of the reactant at time t , C_o is the initial concentration of the reactant and k_{app} is the apparent rate constant. A plot of $\ln(C/C_o)$ versus the irradiation time should give a straight line whose slope corresponds to the apparent pseudo-first-order rate constant, k_{app}. Table (3.8) lists the values of the apparent pseudo-first-order rate constant and half-times, $t^{0.5}$ ($t^{0.5} = 0.693/k_{app}$), for the photodegradation, photodegradation/adsorption and photodegradation/adsorption / TiO_2 of THMs obtained in the present study.

Table (3.7) Apparent Pseudo-first-order Kinetic Rate Constants, k_{app}, Half-times, $t^{0.5}$, and Correlation Coefficient Values, R^2, for the Removal of THMs by Different Processes

Sorbate	Photodegradation			Photodegradation /adsorption			Photodegradation /adsorption / TiO_2		
	$10^4 k_{app}$ (min^{-1})	$t_{0.5}$ (min)	R^2	$10^4 k_{app}$ (min^{-1})	$t_{0.5}$ (min)	R^2	$10^4 k_{app}$ (min^{-1})	$t_{0.5}$ (min)	R^2
$CHBr_3$	752	16.90	0.945	936	20.88	0.997	1065	27.96	0.975
$CHCl_3$	639	23.41	0.839	871	31.64	0.989	940	34.01	0.928
$CHBr_2Cl$	411	35.80	0.968	693	25.03	0.879	738	29.26	0.989
$CHBrCl_2$	358	26.52	0.936	485	23.13	0.976	657	28.04	0.947

As seen from the values of the correlation coefficients, R^2, the results show that the THMs removal did not follow pseudo-first-order kinetics. Hence, the pseudo-second-order kinetic model was used to explain the experimental data obtained. The pseudo-second-kinetic order rate law can be expressed by the following equation[144].

$$t/Q_t = (t / k_{app} Q_o^{\,2}) + (t / Q_o)$$

where Q_o is the total amount of solute present in aqueous solution initially, Q_t is the amount of solute present in aqueous solution after time, t, and k_{app} is the apparent rate constant. Plotting t/Q_t versus the irradiation time, t, should give a straight line from which the apparent

rate constant may be obtained from the value of the intercept with the y-axis. The correlation coefficients listed in Table (3.8) indicate that the process followed pseudo-second-order kinetics. The data listed in Table (3.7) indicate that the half-time for photodegradation alone was considerably greater than that observed for the combination of photodegradation /adsorption and for the combination of photodegradation/adsorption /TiO_2. The apparent THM removal rate, k_{app}, showed a considerable and rapid increase in the case of photodegradation/adsorption /TiO_2 hybrid relative to the individual processes.

Table (3.8) Apparent Pseudo-second-order Kinetic Rate Constants, k_{app}, and Correlation Coefficient Values, R^2, for the Removal of THMs by Different Processes

Sorbate	Photodegradation			Photodegradation /adsorption			Photodegradation /adsorption /TiO_2		
	$10^4 k_{app}$ (min^{-1})	$t_{0.5}$ (min)	R^2	$10^4 k_{app}$ (min^{-1})	$t_{0.5}$ (min)	R^2	$10^4 k_{app}$ (min^{-1})	$t_{0.5}$ (min)	R^2
$CHBr_3$	175	29.3	0.997	256	23.01	0.989	422	33.27	0.989
$CHCl_3$	230	36.02	0.999	312	17.4	0.989	569	18.2	0.997
$CHBr_2Cl$	163	38.06	0.994	275	25.3	0.997	398	36	0.999
$CHBrCl_2$	118	34.44	0.999	146	33.22	0.997	266	24.07	0.999

Table (3.8) indicating the presence of a synergistic effect. Thus, the addition of olive stone activated carbon and olive stone activated carbon with TiO_2 in the presence of UV illumination accelerates the removal of THMs and decreases the decay time. Active carbon and with TiO_2 itself contributes in two ways to the process: (i) it acts a catalyst promoting the degradation of THMs and (ii) as an adsorbent removing the intermediates and by-products arising from the degradation of the THMs.[144]